ETH
Eidgenössische Technische Hochschule Zürich
Swiss Federal Institute of Technology Zurich

Seminar for Applied Mathematics SAM

DG Treatment of Non-Conforming Interfaces in 3D Curl-Curl Problems

R. Casagrande and C. Winkelmann and R. Hiptmair and J. Ostrowski

Research Report No. 2014-32
November 2014

Seminar für Angewandte Mathematik
Eidgenössische Technische Hochschule
CH-8092 Zürich
Switzerland

DG Treatment of Non-Conforming Interfaces in 3D Curl-Curl Problems

Raffael Casagrande, Christoph Winkelmann, Ralf Hiptmair, and Joerg Ostrowski

Abstract We consider 3D Curl-Curl type of problems in the presence of arbitrary, non-conforming mesh-interfaces. The Interior Penalty/Nitsche's Method [1] is extended to these problems for edge functions of the first kind. We present an a priori error estimate which indicates that one order of convergence is lost in comparison to conforming meshes due to insufficient approximation properties of edge functions. This estimate is sharp for first order edge functions: In a numerical experiment the method does not converge as the mesh is refined.

1 Introduction

The Curl-Curl equation,

$$\nabla \times (\mu^{-1} \nabla \times \mathbf{A}) = \mathbf{j}^i, \tag{1}$$

can be used to calculate the magnetic field that originates from a stationary current $\mathbf{j}^i$. Herein μ denotes the magnetic permeability, $\mathbf{A}$ is the magnetic vector potential and the magnetic field is $\mathbf{B} = \nabla \times \mathbf{A}$. The Magnetostatic model (1) is a special case of the temporally gauged Eddy Current model (note that (2) reduces to (1) in static cases, and also in regions with $\sigma = 0$) ,

$$\sigma \frac{\mathrm{d}\mathbf{A}}{\mathrm{d}t} + \nabla \times (\mu^{-1} \nabla \times \mathbf{A}) = \mathbf{j}^i. \tag{2}$$

Raffael Casagrande, Christoph Winkelmann, Ralf Hiptmair
Seminar for Applied Mathematics, ETH Zürich, Rämistr. 101, CH-8092 Zürich,
e-mail: raffael.casagrande@sam.math.ethz.ch, christoph.winkelmann@sam.math.ethz.ch, hiptmair@sam.math.ethz.ch

Joerg Ostrowski
ABB Switzerland Ltd., Corporate Research, Segelhofstrasse 30-34, CH-5405 Baden, Switzerland,
e-mail: joerg.ostrowski@ch.abb.com

In some applications like the simulation of electric machines or magnetic actuators, magnetic fields have to be computed in the presence of moving, rigid parts. Then one may use separate, moving sub-meshes for them in order to avoid remeshing. However, this leads to so-called "sliding interfaces", i.e. meshes with hanging nodes (cf. Fig. 1).

Fig. 1 Initially conforming sub-meshes become non-conforming when the upper sub-mesh starts moving.

Our aim is to construct a method which solves (1) such that the solution is not affected by the "non-conformity" of the sub-meshes at the common interface. This problem has been studied in depth in the framework of so called Mortar Methods where the continuity requirements are incorporated directly into the trial-space [2] or they are enforced by additional Lagrange Multipliers [3]. These approaches have been proven to be successful, but they require the inversion of a full matrix respectively additional unknowns. A related approach uses a primal/dual formulation and couples the systems in a weak sense across the interface [4].

We pursue a different approach that fits into the framework of Discontinuous Galerkin (DG) methods which support non-conforming meshes naturally. A Locally Discontinuous Galerkin scheme for sliding meshes has already been proposed and analyzed in [5]. We will study a simpler method which has it's origins in Nitsche's Method. The idea is to penalize tangential discontinuities along the non-conforming interface, but not in the interior of the subdomains where we use a standard FEM discretization. The method has been analyzed for the Poisson Equation in [1] where it was shown that a symmetric positive definite system matrix results. We aim to extend this idea to (1).

It is important to realize that (1) and (2) (if $\sigma = 0$ anywhere) don't have a unique solution (in the L^2-norm). In this work, we will therefore study the regularized problem,

$$\nabla \times (\mu^{-1} \nabla \times \mathbf{A}) + \varepsilon \mathbf{A} = \mathbf{j}^i, \quad \text{in } \Omega \tag{3}$$

$$\mathbf{n} \times \mathbf{A} = \mathbf{g}_D \quad \text{on } \partial\Omega. \tag{4}$$

Here $\varepsilon > 0$ is the regularization parameter that renders the solution unique. We will discuss the influence and necessity of the regularization term in a future work. Finally we want to point out that the boundary condition (4) implies $(\nabla \times \mathbf{A}) \cdot \mathbf{n} = \mathbf{B} \cdot \mathbf{n} = 0$ on $\partial\Omega$ which reflects the decay of the fields away from the source.

We start our discussion by introducing DG notations (Sect. 2) that we need in order to introduce the interior penalty formulation in Sect. 3. Sect. 3 also analyzes the behavior of the discrete solution as the mesh is refined (h-refinement) and the role of the approximation space is studied. The theoretical results are compared to

numerical experiments in Sect. 4. We finish our discussion by a short conclusion and outlook (Sect. 5).

2 Preliminaries

Before we can introduce the Symmetric Weighted Interior penalty (SWIP) formulation of (3-4) we introduce some definitions and notations:

Subdomains and sub meshes: Let us assume that the domain Ω, on which (3-4) is posed, is a simply connected polyhedron with Lipschitz boundary. Furthermore we assume Ω to be split into two non-overlapping subdomains $\overline{\Omega_1} \cup \overline{\Omega_2} = \overline{\Omega}$. On each subdomain we introduce a sequence of shape regular, simplical meshes in the sense of Ciarlet such that the union $\mathscr{T}_\mathscr{H} = \mathscr{T}_{\mathscr{H},1} \cup \mathscr{T}_{\mathscr{H},2}$ is a *shape and contact regular* mesh sequence (cf. [6], Def. 1.38). It is easy to check that meshes created by the motion of individual sub-meshes (cf. Fig. 1) fit this definition.

Magnetic Permeability: We assume there exists a partition $P_\Omega = \{\Omega_{i,\mu}\}$ such that each $\Omega_{i,\mu}$ is a polyhedron and such that the permeability $\mu > 0$ is constant on each $\Omega_{i,\mu}$. Furthermore the mesh sequence $\mathscr{T}_\mathscr{H}$ is *compatible* with the partition P_Ω: For each $\mathscr{T}_h \in \mathscr{T}_\mathscr{H}$, each element $T \in \mathscr{T}_h$ belongs to exactly one $\Omega_{i,\mu} \in P_\Omega$. I.e. the magnetic permeability is allowed to jump over element boundaries, and in particular over the non-conforming interface $\Gamma = \overline{\Omega}_1 \cap \overline{\Omega}_2$

Polynomial approximation: Later on we will seek our discrete solution in the piecewise polynomial space (cf. [6]),

$$P_3^k(\mathscr{T}_h) := \left\{ p \in L^2(\Omega) \,\middle|\, \forall T \in \mathscr{T}_h,\, p|_T \in P_3^k(T) \right\} \tag{5}$$

where $\mathscr{T}_h \in \mathscr{T}_\mathscr{H}$ and $P_3^k(T)$ is the usual space of polynomials up to degree k on mesh element T. Note that functions of $P_3^k(\mathscr{T}_h)$ are discontinuous across element boundaries.

Mesh Faces, Jump and Average Operators We denote by $\mathscr{F}_h = \mathscr{F}_h^b \cup \mathscr{F}_h^i$ the set of all boundary and inner faces of a given mesh $\mathscr{T}_h$. $\mathscr{F}_T$ stands for all faces of the mesh element $T \in \mathscr{T}_h$. For each mesh face F, *vector valued* function $\mathbf{A}_h \in P_3^k(\mathscr{T}_h)^3$, we define

$$\begin{aligned}
&\text{if } F \in \mathscr{F}_h^i,\, F = \partial T_i \cap \partial T_j: && [\mathbf{A}_h]_T = \mathbf{n}_F \times \left(\mathbf{A}_h|_{T_i} - \mathbf{A}_h|_{T_j} \right), && \text{(jump)}\\
&\text{if } F \in \mathscr{F}_h^b,\, F = \partial T_i \cap \partial \Omega: && [\mathbf{A}_h]_T = \mathbf{n}_F \times \mathbf{A}_h|_{T_i}, &&\\
&\text{if } F \in \mathscr{F}_h^i,\, F = \partial T_i \cap \partial T_j: && \{\mathbf{A}_h\}_\omega = \omega_1\, \mathbf{A}_h|_{T_i} + \omega_2\, \mathbf{A}_h|_{T_j}, && \text{(average)}\\
&\text{if } F \in \mathscr{F}_h^b,\, F = \partial T_i \cap \partial \Omega: && \{\mathbf{A}_h\}_\omega = \mathbf{A}_h|_{T_i}. &&
\end{aligned}$$

Here $\mathbf{n}_F$ always points from T_i to T_j and $\omega_i \in [0,1]$ such that $\omega_1 + \omega_2 = 1$.

3 Symmetric Weighted Interior Penalty (SWIP) Formulation

We chose an arbitrary subspace $V_h \subseteq P_3^k(\mathscr{T}_h)^3$ as discrete test and trial space, and use integration by parts (cf. [6, 7] for details) to arrive at the SWIP formulation of (3): Find $\mathbf{A}_h \in V_h$ such that

$$a_h^{\mathrm{SWIP}}(\mathbf{A}_h, \mathbf{A}'_h) + \varepsilon \int_\Omega \mathbf{A}_h \cdot \mathbf{A}'_h = \ell_h(\mathbf{A}'_h) \qquad \forall \mathbf{A}'_h \in V_h \tag{6}$$

with

$$\begin{aligned} a_h^{\mathrm{SWIP}}(\mathbf{A}_h, \mathbf{A}'_h) = &\int_\Omega \left(\mu^{-1}\nabla\times\mathbf{A}_h\right)\cdot\left(\nabla\times\mathbf{A}'_h\right) - \sum_{F\in\mathscr{F}_h}\int_F \left\{\mu^{-1}\nabla\times\mathbf{A}_h\right\}_\omega \cdot \left[\mathbf{A}'_h\right]_T \\ &- \sum_{F\in\mathscr{F}_h}\int_F \left\{\mu^{-1}\nabla\times\mathbf{A}'_h\right\}_\omega \cdot [\mathbf{A}_h]_T + \sum_{F\in\mathscr{F}_h} \frac{\eta\gamma_{\mu,F}}{h_F}\int_F [\mathbf{A}_h]_T \cdot \left[\mathbf{A}'_h\right]_T, \end{aligned} \tag{7}$$

$$\begin{aligned} \ell_h(\mathbf{A}'_h) = &\int_\Omega \mathbf{j}^i \cdot \mathbf{A}'_h - \sum_{F\in\mathscr{F}_h^b}\int_F \left\{\mu^{-1}\nabla\times\mathbf{A}'_h\right\}_\omega \cdot (\mathbf{n}\times\mathbf{g}_D) \\ &+ \sum_{F\in\mathscr{F}_h^b} \frac{\eta\gamma_{\mu,F}}{h_F}\int_F \left[\mathbf{A}'_h\right]_T \cdot (\mathbf{n}\times\mathbf{g}_D). \end{aligned} \tag{8}$$

where h_F denotes the diameter of face F and η is the penalty parameter. The weights are chosen as

$$\gamma_{\mu,F} := \frac{2}{\mu_1+\mu_2}, \qquad \omega_1 := \frac{\mu_1}{\mu_1+\mu_2}, \qquad \omega_2 := \frac{\mu_2}{\mu_1+\mu_2}.$$

Remark If $V_h \subseteq \mathbf{H}(\mathbf{curl})$, then all inner tangential jumps in (7) will drop out and only jumps at the boundary remain. I.e. we are left with a standard FEM formulation where the inhomogeneous boundary conditions (4) are enforced in a weak sense.

3.1 A Priori Error Estimate

Using the theory of DG Methods one can derive the following error estimate [9]:

Theorem 1. *Let $\mathbf{A} \in V^* := \mathbf{H}(\mathbf{curl},\Omega)\cap H^2(P_\Omega)^3$ be a solution of the strong formulation (3-4) (in the sense of distributions) and let $\mathbf{A}_h \in V_h \subseteq P_3^k(\mathscr{T}_h)^3$ solve the variational formulation (6). Then there exist constants $C>0$, $C_\eta>0$, both independent of h, μ, such that for $\eta > C_\eta$,*

$$\|\mathbf{A}-\mathbf{A}_h\|_{SWIP} < C \inf_{\mathbf{v}_h\in V_h} \|\mathbf{A}-\mathbf{v}_h\|_{SWIP,*}, \tag{9}$$

and the discrete problem (6) is well-posed.

The associated function spaces and norms are defined by

$$
\begin{aligned}
H^2(P_\Omega)^3 &:= \left\{ \mathbf{A} \in L^2(\Omega)^3 \middle| \forall \Omega_{i,\mu} \in P_\Omega : \ \mathbf{A}|_{\Omega_{i,\mu}} \in H^2(\Omega_{i,\mu})^3 \right\}, \\
\|\mathbf{A}\|^2_{\mathrm{SWIP}} &:= \|\mu^{-1/2}\nabla\times\mathbf{A}\|^2_{L^2(\Omega)} + \|\varepsilon^{1/2}\mathbf{A}\|^2_{L^2(\Omega)} + \sum_{F\in\mathscr{F}_h} \frac{\gamma_{\mu,F}}{h_F} \| [\mathbf{A}]_T \|^2_{L^2(F)}, \quad (10) \\
\|\mathbf{A}\|^2_{\mathrm{SWIP},*} &:= \|\mathbf{A}\|^2_{\mathrm{SWIP}} + \sum_{T\in\mathscr{T}_h} h_T \|\mu^{-1/2}\, \nabla\times\mathbf{A}|_T \|^2_{L^2(\partial T)}.
\end{aligned}
$$

Theorem 1 tells us that the total error is bounded by the best approximation error. In the following we will bound the best approximation error in the $\|\cdot\|_{\mathrm{SWIP},*}$ norm for two concrete choices of V_h.

Edge Functions of the first kind In this section we assume $V_h = R^k(\Omega_1) \oplus R^k(\Omega_2) \subset P_3^k(\mathscr{T}_h)$, where R^k is the space of k-th order edge functions (cf. [8], Sect. 5.5) of the first kind. The following polynomial approximation result gives a bound on the right-hand side of (9):

Theorem 2. *Assume the exact solution $\mathbf{A} \in V := \mathbf{H}(\mathbf{curl},\Omega) \cap H^{s+1}(\Omega_1 \oplus \Omega_2)^3$ with integer $1 \le s \le k$, then there exists a projector $\pi_h : V \mapsto V_h$ such that*

$$
\|\mathbf{A} - \pi_h\mathbf{A}\|_{SWIP,*} < Ch^{s-1} \left(\|\mathbf{A}\|_{H^{s+1}(\Omega_1)^3} + \|\mathbf{A}\|_{H^{s+1}(\Omega_2)} \right).
$$

Where C is independent of h.

Sketch of Proof. The approximation space V_h consists of two standard edge element spaces in Ω_1, Ω_2. We can thus use the standard projection operator r_h, as it is defined in [8], for edge functions on Ω_1, Ω_2 to compose our global projection operator π_h:

$$
\pi_h(\mathbf{A}) := \left(r_h\left(\mathbf{A}|_{\Omega_1} \right), r_h\left(\mathbf{A}|_{\Omega_2} \right) \right).
$$

Next, we note that all the tangential jumps in (7) and (10) that lie on interior, conforming faces drop out and only jumps over $F \in \mathscr{F}_h^{b,\Gamma} := \mathscr{F}_h^b \cup \left\{ F \in \mathscr{F}_h^i \middle| F \subset \overline{\Omega}_1 \cap \overline{\Omega_2} \right\}$ remain. Thus,

$$
\begin{aligned}
\|\mathbf{A} - \pi_h\mathbf{A}\|^2_{\mathrm{SWIP},*} &= \|\mu^{-1/2}\nabla\times(\mathbf{A}-\pi_h\mathbf{A})\|^2_{L^2(\Omega)} + \|\varepsilon^{1/2}(\mathbf{A}-\pi_h\mathbf{A})\|^2_{L^2(\Omega)} \\
&\quad + \sum_{F\in\mathscr{F}_h^{b,\Gamma}} \frac{\gamma_{\mu,F}}{h_F} \| [\mathbf{A}-\pi_h\mathbf{A}]_T \|^2_{L^2(F)} + \sum_{T\in\mathscr{T}_h} h_T \|\mu^{-1/2}\nabla\times(\mathbf{A}-\pi_h\mathbf{A})\|^2_{L^2(\partial T)}, \\
&= T_1 + T_2 + T_3 + T_4.
\end{aligned}
$$

The terms T_1, T_2, T_4 are easily bounded in terms of $O(h^{2s})$ by standard polynomial approximation results (cf. Thm. 5.41 in [8]). However, for T_3 we have to use Lemma 5.52 in [8] to achieve a rate $O(h^{2s-2})$ which unfortunately dominates the other terms. The fact that the error contribution T_3 is confined to a neighborhood of the interface, respectively the boundary, does not help, because the solution may be concentrated there as well.

Piecewise Polynomials For the sake of completeness we shortly present an approximation result for the case $V_h = P_3^k(\mathscr{T}_h)$:

Theorem 3. *Assume the exact solution* $\mathbf{A} \in V := \mathbf{H}(\mathbf{curl}, \Omega) \cap H^{s+1}(P_\Omega)^3$ *with integer* $1 \leq s \leq k$*, then there exists a projector* $\pi_h^P : V \mapsto V_h$ *such that*

$$\|\mathbf{A} - \pi_h^P \mathbf{A}\|_{SWIP,*} < Ch^s \|\mathbf{A}\|_{H^{s+1}(P_\Omega)^3}$$

where C is independent of h.

For the proof of this theorem we refer the reader to the proof of Thm. 3.21 in [7]. The important point is that piecewise polynomials $P_3^k(\mathscr{T}_h)$ yield the expected rate of convergence because they span the full polynomial space.

4 Numerical Results

We consider a 3D sphere with radius 1 that is split into two half-spheres which are then meshed individually (Fig. 2). We impose the analytical solution $\mathbf{A} = (\sin y, \cos z, \sin x)$ and choose $\mathbf{j}^i$, $\mathbf{g}_D$ correspondingly ($\mu = 1$, $\varepsilon = 10^{-6}$).

Figure 3 shows the error for a sequence of quasi-uniform meshes which approximate the boundary linearly. We can see that piecewise polynomials yield always the expected rate of converge, $O(h)$, but this does not hold for edge functions: For $V_h = R^1(\Omega_1) \oplus R^1(\Omega_2)$ the error fluctuates significantly depending on the angle (see Fig. 4) and for $\theta = 2.86$ (solid line) no convergence is observed. This shows that the estimate in Thm. 2 is sharp for $k = 1$. For $k = 2$ we would expect $O(h)$ convergence but for all configurations we observe a rate of order at least $O(h^{1.5})$ because in this experiment the solution is not concentrated at the interface/boundary: T_3 decays faster than in the worst case.

Finally, Figure 4 shows the relative error for different rotation angles for a fixed mesh width h. This confirms the previous result in that the error for $V_h = R^1(\Omega_1) \oplus R^1(\Omega_2)$ depends on the geometry of the overlapping meshes. For $V_h = P^1(\mathscr{T}_h)$, respectively $V_h = R^2(\Omega_1) \oplus R^2(\Omega_2)$ the error does not depend on θ.

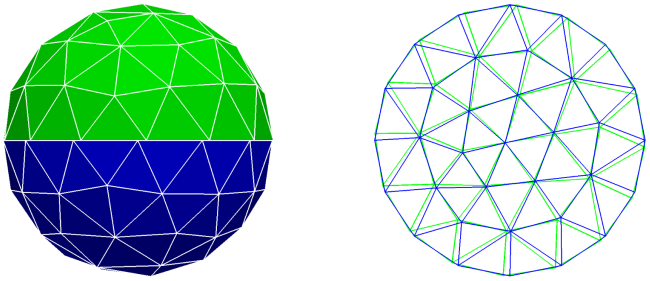

Fig. 2 The meshes for the two half spheres. The upper hemi-sphere is turned against the lower hemisphere by $\theta = 2.86$ degrees to create a non-conforming mesh.

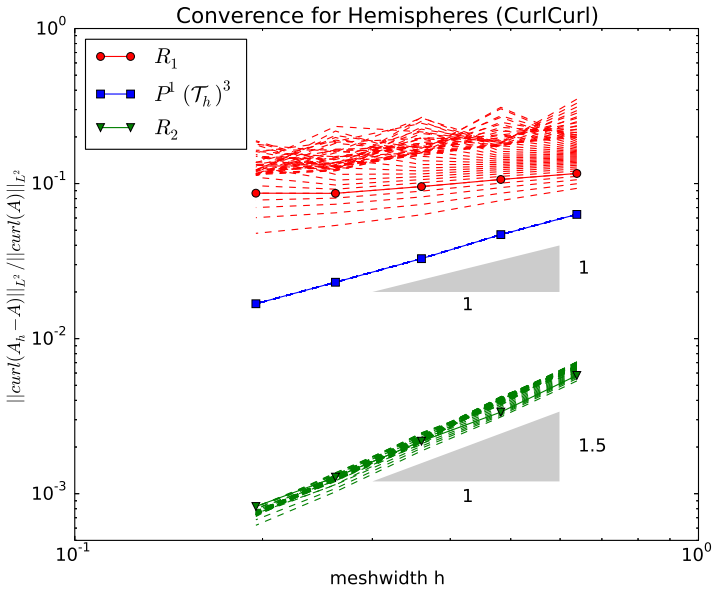

Fig. 3 The relative $\mathbf{H}(\mathbf{curl})$ error vs. mesh size h for rotation angle $\theta = 2.86$ degrees (solid lines). The dashed gray lines correspond to $\theta = 90n/(50\pi)$ degrees, $n \in \{0, 1, \ldots, 49\}$

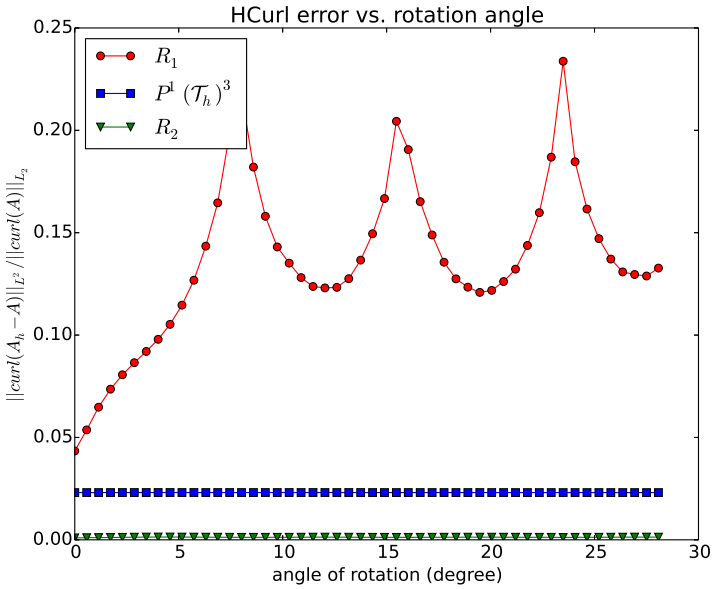

Fig. 4 The relative $\mathbf{H}(\mathbf{curl})$ error vs. the rotation angle for $h = 0.261$.

5 Conclusion and Outlook

We have shown that a straightforward generalization of the Interior Penalty/Nitsche's Method to 3D Curl-Curl problems does not yield the expected rate of convergence if edge functions of the first kind are used. Generally one order of convergence is lost, i.e. for k-th order edge functions we observe $O(h^{k-1})$ convergence as the mesh is refined. The reason for this is that R^k doesn't span the full polynomial space P^k. Moreover, the result is sharp for $k = 1$, i.e. the method fails completely for first order edge functions. This problem can be cured by using either the full polynomial space P^1 or by using second order edge functions R^2.

The proposed SWIP scheme leads to a sparse, symmetric positive definite matrix which yields, together with the conjugate gradient method, a fast and robust solution scheme. Furthermore μ can be discontinuous across the non-conforming interface.

Outlook The proof of Thm. 2 suggests that it suffices to use 2nd order edge functions solely in elements adjacent to the non-conforming interface to achieve $O(h)$ convergence. This is easily implemented using hierarchical edge functions [10] and reduces the required number of degrees of freedom drastically. Another open question is whether the problem can still be solved using CG if the regularization term in (3) is dropped because the system matrix then becomes positive semi-definite and the right-hand side is no longer in its range. Also, it is unclear whether the SWIP bilinear form offers a spectrally accurate discretization of the Curl-Curl operator [11] for $\varepsilon = 0$ and thus the convergence rate of CG may deteriorate as $h \to 0$.

References

1. Stenberg, R.: Mortaring by a method of JA Nitsche. Computational mechanics (1998)
2. Rapetti, F., Maday, Y., Bouillault, F., Razek, A.: Eddy-Current Calculations in Three-Dimensional Moving Structures IEEE Transactions on Magnetics, **38.2**, 613-616 (2002)
3. Wohlmuth, I.: Discretization Methods and Iterative Solvers Based on Domain Decomposition Springer, Berlin Heidelberg (2001)
4. Rodriguez, A.A., Hiptmair, R., Valli, A.: A hybrid formulation of eddy current problems Numerical Methods for Partial Differential Equations, **21.4**, 742-763 (2005)
5. Perugia, I., Schötzau, D.: On the Coupling of Local Discontinuous Galerkin and Conforming Finite Element Methods Journal of Scientific Computing, **16.4**, 411-433, (2001)
6. Di Pietro, D.A., Ern, A.: Mathematical aspects of discontinuous Galerkin methods Springer, Heidelberg, London, New York (2012)
7. Casagrande, R.: Sliding Interfaces for Eddy Current Simulations Master's thesis, ETH Zürich, Zürich (2013)
8. Monk, P.: Finite element methods for Maxwell's equations. Oxford University Press, New York (2003)
9. Casagrande, R.: An a priori error estimate for interior penalty discretizations of the Curl-Curl operator on non-conforming meshes. SAM Report, ETH Zürich, Zürich (2014)
10. Bergot, M., Duruflé, M.: High-order optimal edge elements for pyramids, prisms and hexahedra Journal of Computational Physics, **232**, 189-213, (2013)
11. Buffa, A., Houston, P., Perugia, C.: Discontinuous Galerkin computation of the Maxwell eigenvalues on simplicial meshes Journal of Comp. and Applied Math., **204**, 317-333, (2007)

Recent Research Reports

Nr.	Authors/Title

2014-22 S. Mishra and Ch. Schwab and J. Sukys
Multi-Level Monte Carlo Finite Volume methods for uncertainty quantification of acoustic wave propagation in random heterogeneous layered medium

2014-23 J. Dick and Q. T. Le Gia and Ch. Schwab
Higher order Quasi Monte Carlo integration for holomorphic, parametric operator equations

2014-24 C. Sanchez-Linares and M. de la Asunci on and M. Castro and S. Mishra and J. Šukys
Multi-level Monte Carlo finite volume method for shallow water equations with uncertain parameters applied to landslides-generated tsunamis

2014-25 R.N. Gantner and Ch. Schwab
Computational Higher Order Quasi-Monte Carlo Integration

2014-26 C. Schillings and Ch. Schwab
Scaling Limits in Computational Bayesian Inversion

2014-27 R. Hiptmair and A. Paganini
Shape optimization by pursuing diffeomorphisms

2014-28 D. Ray and P. Chandrashekar and U. Fjordholm and S. Mishra
Entropy stable schemes on two-dimensional unstructured grids

2014-29 H. Rauhut and Ch. Schwab
Compressive sensing Petrov-Galerkin approximation of high-dimensional parametric operator equations

2014-30 M. Hansen
A new embedding result for Kondratiev spaces and application to adaptive approximation of elliptic PDEs

2014-31 F. Mueller and Ch. Schwab
Finite elements with mesh refinement for elastic wave propagation in polygons